



Migration of tidal sand waves  
by Leo C. van Rijn; [www.leovanrijn-sediment.com](http://www.leovanrijn-sediment.com)

Contents

1. Introduction
2. Mechanism of sand wave migration
3. Simple sand wave migration model (SEDUBE.xls)
  - 3.1 Approach
  - 3.2 Adjustment of sediment concentrations
  - 3.3 Slope effects
  - 3.4 Bed level changes
  - 3.5 Input data
4. Sand waves in coastal seas
  - 4.1 Sand wave example
  - 4.2 Artificial sand wave near Hook of Holland, The Netherlands
5. References

1. Introduction

Tidal sand waves with a length scale of about 1 km are common features on the Dutch shoreface of the North sea (depth range of 10 to 50 m), see Van de Meene (1994) and Hulscher (1996a,b).

Generally, these bed features are observed in conditions with relatively strong currents in the range of 0.5 to 1 m/s and sediments in the medium sand size range of 0.2 to 0.5 mm. These sand waves with a maximum height of the order of 5 m are dynamically active and show migration rates of the order of a few metres per year. Generally, the sand wave crests are approximately normal to the tidal current. These sand waves which occur in large fields in the offshore coastal zone offer an easily available source of sand for mining purposes and therefore get increasingly attention of coastal managers.

Two types of models are generally used to study the behaviour of large-scale bed features: stability models and morphodynamic models, see for overview Hulscher (1996a) and Vittori et al. (2005).

The stability-based models can be used to determine the stability properties of the sea bed with respect to arbitrary disturbances. Typically, stability models provide information on the time development of the sea bed forms like the wave height and the wave length for given hydrodynamic and morphodynamic conditions. Traditionally, such models have been used to study the possible formation of large scale bedforms, to predict their main geometrical characteristics and to provide a physical explanation of their appearance. Linear stability models yield the bed wave mode (wavelength and crest orientation) which will grow fastest and the growth rate of this mode, indicating the morphological time scale. Non-linear stability models involving the interaction of unstable modes are required to obtain information of the height and shape of the bed wave patterns. Huthnance (1982) was the first to develop a simplified linear stability model to disclose the mechanism originating open shelf sand banks.

A basic restriction of the stability models is that the sand wave shape is sinusoidal, the sand wave height is relatively small and strictly infinitesimal. Generally, the bed load and suspended load transport are taken into account using rather simple transport equations; the entrainment and transportation of the suspended sediments (lag effects) requiring the application of the advection-diffusion equation for the sediment concentration usually is neglected. The same holds for the effect of the orbital wave motion on the suspended sediment transport. Usually, the effect of short surface waves on the sediment transport process is neglected in stability model approaches.

The morphodynamic models are based on the numerical solution of the three-dimensional shallow water equations in combination with a surface wave propagation model (wind waves) and the advection-diffusion equation (to include lag effects) for the sediment particles with on-line bed updating after each time step (Tonnon et al., 2007; Lesser et al. 2004; Van Rijn, 1993; 2006). A major advantage of this approach is that many effects acting on uniform, cohesionless sediment particles moving along tidal sand waves are included,



which however requires a relatively large computational effort restricting 3D model application to a time span of the order of 10 years at present state of computer technology. Finally, it is noted that numerical morphodynamic models are very well suited to simulate the transient behaviour of sand waves of arbitrary shape on the medium term time scale of 10 years in contrast to stability-based models which are more aimed at the long-term behaviour of idealized wave shapes for strongly schematized forcing conditions. In this note, it is shown that sand wave migration can also be modelled using a very simple approach.

## 2. Mechanism of sand wave migration

An essential feature to be modelled is the adjustment of the velocity profiles when the flow passes the sand wave. In unidirectional flow the velocity profiles have a different shape at both sides of the crest of the sand wave; the velocity profiles upstream of the sand wave crest are characterized by increasing velocities in the near-bed zone (bulged shape due to decreasing water depth), while downstream of the crest the velocity profiles are characterized by reduced velocities in the near-bed zone (dipped shape due to increasing water depth and deceleration processes), see **Figure 2.1**.

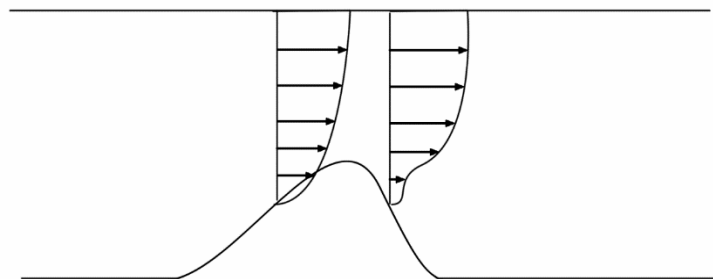


**Figure 2.1** Velocity profiles over sand wave (qualitative sketch for unidirectional flow)

In the case of tidal flow, the direction of the flow changes with the turning of the tide which has its consequences on the time-averaged (residual) velocity profiles at both sides of the sand wave. At maximum flood and maximum ebb flow, the velocity profiles show increased velocities at the upstream flank and reduced velocities at the downstream flank. As the flow during flood and ebb is in opposite direction, the upstream and downstream locations are at opposite sides of the sand waves crest; the bulged velocity profiles change to dipped velocity profiles when the flow reverses. The time-averaged (residual) velocity profiles at both flanks therefore show a vertical distribution as given in **Figure 2.2**; at both flanks the time-averaged (residual) near-bed velocities are directed toward the sand wave crest. This can be interpreted as a vertical circulation cell.

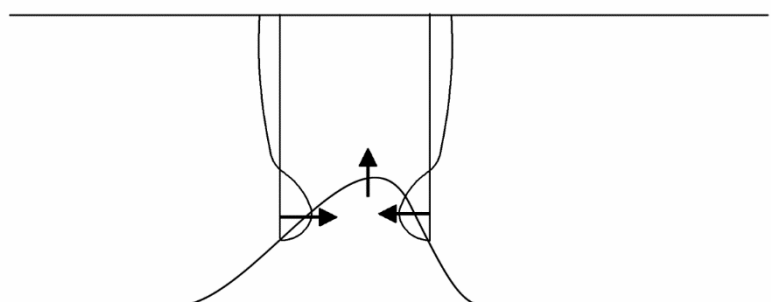


**Figure 2.2** Time-averaged (residual) velocity profiles at flanks of the sand wave.



This mechanism results in vertical growth of the sand wave when bed load transport is dominant; the particles remain in the crest region of the sand wave and are transported towards the sand wave crest. When suspended-load transport higher in the water column is dominant, the sediment particles can be transported beyond the crest region towards the sides of the sand wave resulting in flattening of the sand wave. These effects can only be represented by using a three dimensional model to resolve the vertical structure of the flow accelerating and decelerating over the sand waves.

Another important effect during tidal flow is the continuously changing water depth. The tidal range with decreasing water depths during ebb and increasing water depths during flood affects velocities, transport rates and morphology. The bed shear stress depends on the water depth; the bed shear stress will be larger during ebb flow with shallower water depth at the same depth-averaged velocity.

The effect of waves on the bed-shear stress and sand transport also depends on the water depth. Waves in shallower water depth intensify the stirring action of the oscillatory fluid motion in the near-bed region which leads to larger sediment concentrations and larger transports; with shallower water the effect will be greater and transports will be larger. Thus, assuming equal depth-averaged ebb-velocities and flood-velocities, the transport rates in ebb direction (at upstream flank) are larger than the transport rates in flood direction due to both larger bed shear stresses and increased wave action during ebb.

### 3. Simple sand wave migration model (SEDTUBE.xls)

#### 3.1 Approach

An arbitrary streamtube can be defined by specifying the width and water depth along the streamtube ( $s$ -direction) as input data. By prescribing the widths and water depths along the tube (**Figure 3.1.1**), the depth-averaged velocity can be prescribed (manipulated), as the discharge in the streamtube is constant, resulting in  $u_s = (Q/b_s h)$ .

The width data can be obtained from a detailed mathematical model, from laboratory or field measurements.

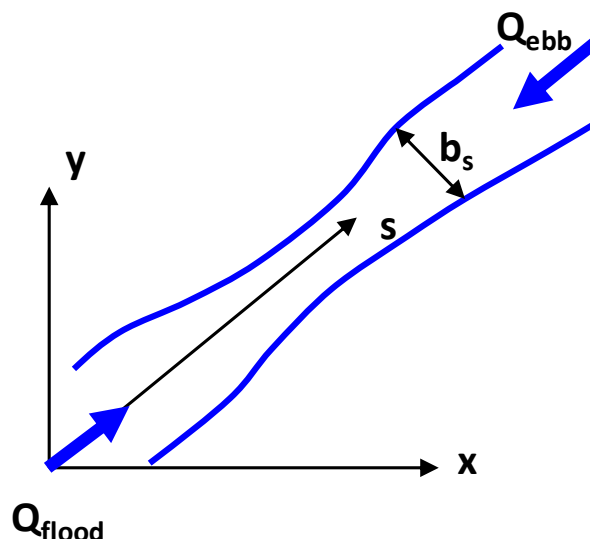


**Figure 3.1.1** Plan view of arbitrary streamtube with varying width  $b_s$  and waterdepth  $h$



### 3.2 Adjustment of sediment concentrations

The adjustment of the depth-averaged sand concentration and the suspended sand transport ( $Q_s = c Q$ ) in a streamtube can be approximated by:

$$dc_x/dx = -A(c_x - c_{x,eq}) \text{ or, } dQ_{s,x}/dx = -A(Q_{s,x} - Q_{s,x,eq})$$

with:

- $c$  = depth-averaged sediment concentration,
- $c_{eq}$  = depth-averaged equilibrium sediment concentration,
- $Q$  = fluid discharge in streamtube (constant),
- $Q_s$  = sediment transport in streamtube (in kg/s),
- $Q_{s,eq}$  = equilibrium sediment transport in streamtube (in kg/s),
- $A$  = adjustment coefficient (in  $m^{-1}$ ).

Using an upwind scheme, the equations can be approximated by:

$$\begin{aligned} Q_{s,x} &= Q_{s,x-\Delta x} + \Delta Q_s \\ Q_{s,x} &= Q_{s,x-\Delta x} + [-A(Q_{s,x} - Q_{s,x,eq}) \Delta x] \\ Q_{s,x} &= [1/(1 + A \Delta x)] [Q_{s,x-\Delta x} + (A Q_{s,x,eq}) \Delta x] = [1/(1 + A \Delta x)] [Q_{s,x-\Delta x}] + [1/(1 + 1/(A \Delta x))] [Q_{s,x,eq}] \end{aligned}$$

with:  $\Delta x$  = grid size.

If  $A$  approaches infinity, it follows that:  $Q_{s,x} \cong Q_{s,x,eq}$ ; If  $A$  approaches zero:  $Q_{s,x} \cong Q_{s,x-\Delta x}$ .

The adjustment factor ( $A$ ) has been determined from computed results for a wide range of conditions based on a detailed suspended transport model (SUTRENCH-model; Van Rijn 1987), yielding:

$$A = 0.1(1/h)(w_s/u_*)(1+2w_s/u_*)(1+H_s/h)^2$$

with:

- $h$  = flow depth,
- $w_s$  = fall velocity of suspended sediment,
- $u_*$  = bed-shear velocity due to currents and waves ( $= u_e g^{0.5}/C$ ),
- $C = 5.75 g^{0.5} \log(12h/k_s)$  = Chézy coefficient,
- $k_s$  = effective bed roughness height of Nikuradse,
- $Q_{s,eq}$  = equilibrium sediment transport,
- $u_e$  = effective velocity =  $u + 0.5U_{s,on}$ ,
- $u$  = depth-averaged flow velocity,
- $U_{s,on}$  = peak orbital velocity near the bed (based on linear wave theory using significant wave height  $H_s$ ),
- $H_s$  = significant wave height.

The adjustment of the suspended transport proceeds relatively rapid in the presence of waves (see effect of  $H_s/h$  parameter). Larger  $A$ -values (larger fall velocity, smaller bed-shear velocity, larger relative wave height) lead to more sedimentation at the upstream side slope and to less sedimentation in the middle of channel (more rapid adjustment to equilibrium conditions).

The equilibrium transport rates are represented by simple engineering formulations related to the bulk flow parameters (depth-averaged flow velocity, wave height), which can be adjusted by a calibration coefficient  $K$  ( $K=1$  = default value;  $K=0.5$  is the best estimate for North Sea conditions with fine sand of about  $200 \mu m$ ), see Van Rijn 1984, 1987, 1993, 2006, 2007.



### 3.3 Slope effects

A rapidly varying bed level (and water depth) along the streamtube has a strong effect on the local sediment transport, as follows:

- the near-bed flow velocities, the bed-shear stresses and sediment transport rates are reduced at downsloping zones and increased at upsloping zones (**Figure 3.3.1**), which cannot be represented by the SEDTUBE-model;
- the bed load transport increases along a downsloping zone and reduces along an upsloping zone due to the action of the slope-related gravity component.

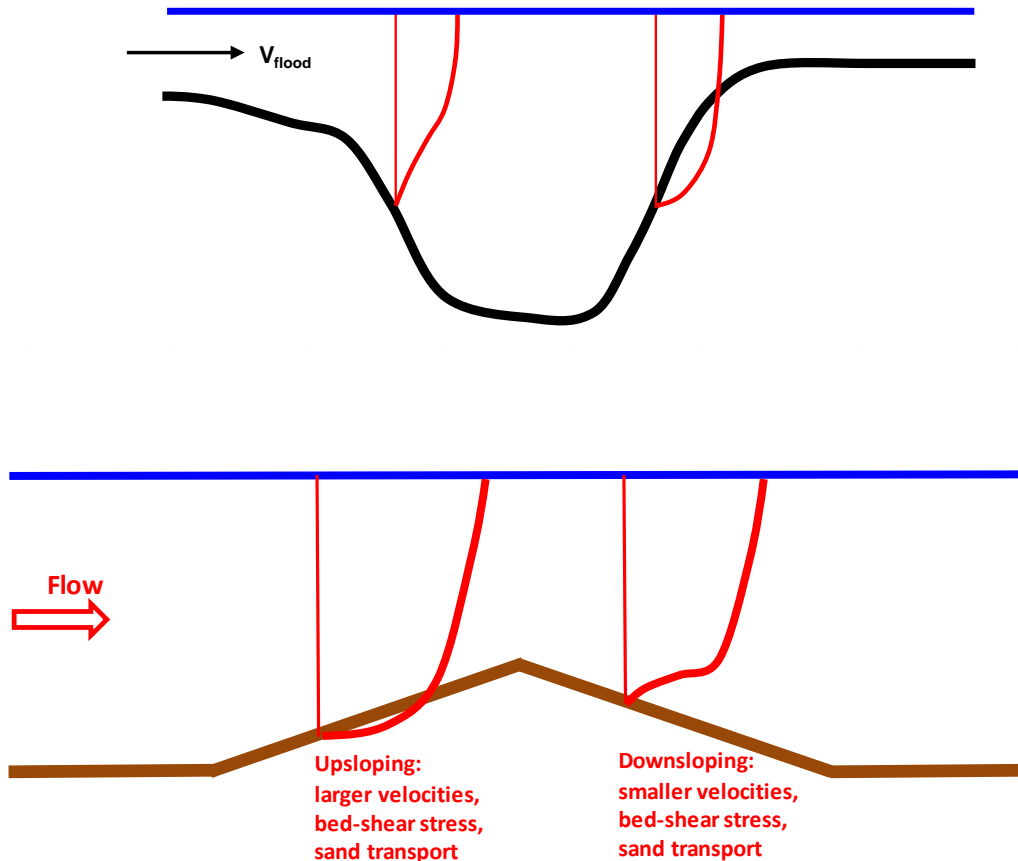


**Figure 3.3.1** Modification of velocity profiles crossing channel (upper) and sand wave (lower)

In cases with dominant suspended load transport, the modification of the near-bed velocities and its effect on the local sediment transport is most important. To include this effect to some extent, a slope factor is introduced as a multiplication factor acting on the local sediment transport (bed load+suspended load). The slope factor representing the velocity modification effect, reduces the sediment transport at downsloping zones and increase the transport at upsloping zones. The slope factor reads as:

$$f_{slope} = 1 - 10 \delta_{slope} \tan \gamma \quad \text{and} \quad f_{slope, maximum} = 1.1; \quad f_{slope, minimum} = 0.7$$

with:

$\tan \gamma = \Delta z_b / \Delta x = \Delta h / \Delta x =$  side slope angle (+ =downsloping flow; - =upsloping flow);

$z_b =$  bed level to datum;  $h =$  water depth;

$\delta_{slope} =$  input value ( $\delta_{slope} = 0 =$  no effect;  $\delta_{slope} = 0.5 =$  slight effect;  $\delta_{slope} = 1 =$  maximum effect).



### 3.4 Bed level changes

The bed level changes are described by:

$$b\Delta z_b/\Delta t + [(1-\varepsilon)\rho_s]^{-1} [\Delta(bq_{total})/\Delta s] = 0$$

$$\Delta z_{b,i,t+\Delta t} = - [2\Delta s (1-\varepsilon)\rho_s]^{-1} \Delta t [b_{i+1}q_{total,i+1,t} - b_{i-1}q_{total,i-1,t}] + 0.5 \gamma_s [z_{b,i+1,t} - 2z_{b,i,t} + z_{b,i-1,t}]$$

with:

$z_b$ = bed level to datum,

$b$ = width of streamtube,

$s$ = coordinate along streamtube,

$q_b$ = bed load transport (in kg/m/s),

$q_s$ = suspended load transport (in kg/m/s),

$q_{total}=q_b+q_s$ = total sediment transport (kg/m/s),

$\varepsilon$ = porosity of bed material deposits,

$\rho_s$ = sediment density,

$\gamma_s$ = smoothing-coefficient (0.01-0.001).

### 3.5 Input data

The input data are:

- $b$ , streamtube width along streamtube [m];
- $h$ , waterdepth to datum along the streamtube [m];
- $v$ , depth-averaged flow velocity at  $x=0$ ; two values: flood and ebb velocity in tidal flow [m/s];
- $\Delta h$ , water level to datum [m];
- $H_s$ , significant wave height at  $x=0$ ; two values in tidal flow [m];
- $T_p$ , peak wave period [s];
- $d_{50}$  and  $d_{90}$ , characteristic diameters of bed material [m];
- $w_s$ , settling velocity of suspended sediment [m/s];
- $p_{mud}$ , percentage mud in bed material [-];
- $\rho_w$ , density of seawater [kg/m<sup>3</sup>];
- $\rho_s$ , density of sediment [kg/m<sup>3</sup>];
- $\nu$ , kinematic viscosity of seawater [m<sup>2</sup>/s];
- $k_s$ , bed roughness height [m];
- $\varepsilon$ , porosity of bed material [-];
- $\delta_{slope}$ , slope factor [-];
- $K$ , calibration coefficient of sediment transport formula [-];
- $\Delta t$ , time step [hours];
- number of time steps per half tide (eb/flood); duration flood is equal to duration ebb;
- total number of tides;
- grid size and initial water depth values across the channel.



#### 4. Sand waves in coastal seas

##### 4.1 Sand wave example

As a practical example, the migration of tidal sand waves with an initial height of 2 m and an initial length of 300 m is computed. The input data are (Table 4.1.1):

- tidal flow over a sand bar with  $v_{\text{flood}}=0.7$  m/s and  $v_{\text{ebb}}=0.6$  m/s;
- mean water depth= 14 m to mean sea level;
- tidal range= 2 m;
- waves  $H_s= 1.5$  m and  $T_p= 7$  s during 100% of the time;
- sediment  $d_{50}= 0.35$  mm.

Figure 4.1.1 and 4.1.2 show the computed bed level after 1 year and 5 years with and without slope effects. Excluding the slope factor, the sand bars are strongly flattened. Including the slope factor, the sand bars are slightly steepened. The computed annual migration rate is of the order of 40 m/year (including the slope factor).

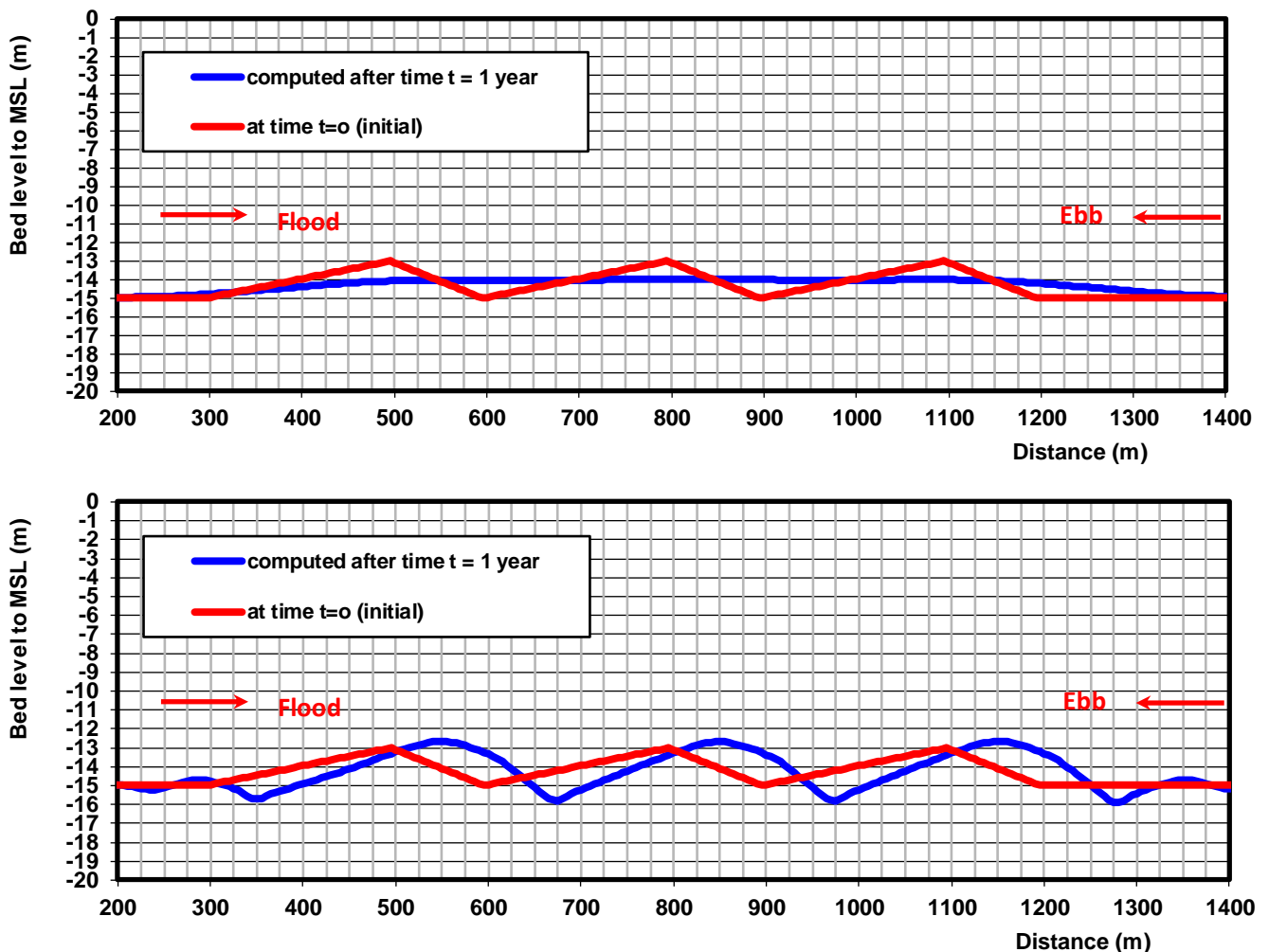


Figure 4.1.1 Computed bed evolution of sand bar after 1 years;  
upper= without slope factor; lower= with slope factor

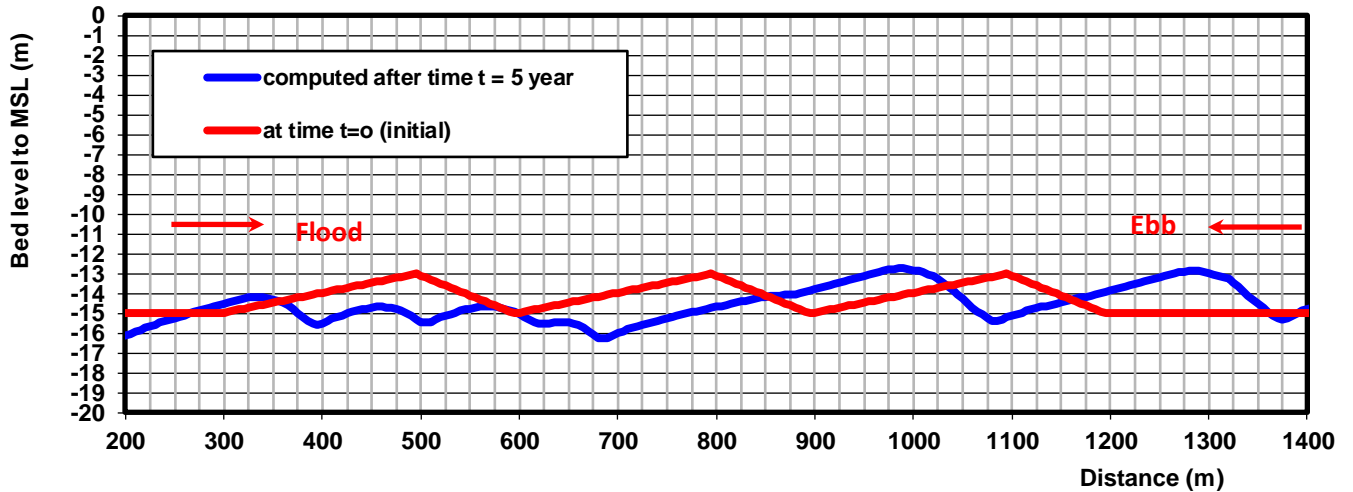


Figure 4.1.2 Computed bed evolution of sand bar after 5 years with slope factor

Depth-averaged velocity at x=0	0.7	0.6 (m/s)
Tidel level	1	-1 (m)
Wave height	1.5	1.5 (m)
Wave period	7	7 (s)
d50 of sand fraction		0.00035 (m)
d90 of sand fraction		0.0006 (m)
Fraction of mud in bed (range of 0 to 0.2)		0.05 (-)
Fluid density		1020 (kg/m <sup>3</sup> )
Sediment density		2650 (kg/m <sup>3</sup> )
Kinematic viscosity		0.000001 (m <sup>2</sup> /s)
Ws suspended sand		0.045 (m/s)
Bed Roughness ks		0.01 (m)
Porosity of bed material p		0.4 (-)
Calibration factor sand transport		0.5 (-)
Calibration factor critical velocity		1 (-)
Slope factor (0 to 1; Default=0=no effect)		1 (-)
Smoothing factor bed levels		0.01 (-)
Flow Duration Dt		16 (hours)
Grid size DX		5 (m)
Coefficient of adjustment factor (range 0.05-0.2)		0.2 (-)
Number of time steps for half a tide		1 (-)
Total number of complete tides (= 2 half tides)		180 (-)

Table 4.1.1 Input data of SEDTUBE-model for sand wave example





#### 4.2 Artificial sand wave near Hoek van Holland, The Netherlands

In the period 1982 to 1986, an artificial sand wave was created by dumping approximately 3.5 million m<sup>3</sup> sand (Van Woudenberg, 1996; Tonnon et al. 2007) which was dredged from the shipping channel to Rotterdam harbour, onto the shoreface (depths between -15 and -23 m to MSL) at the location Hoek van Holland immediately north of the approach channel to the port of Rotterdam, see **Figure 4.2.1**.

The composition of (dumped) sand is similar to that of ambient sediment. The sand wave is more or less perpendicular to the coast, the sand wave dimensions just after creation were: length of about 3600 m; toe width between 250 and 370 m; height between 1.3 and 4 m; slopes between 1:50 and 1:100 on the south flank and between 1:20 and 1:50 on the north flank; d<sub>50</sub> between 0.15 and 0.45 mm. The landward end of the sand wave is about 6300 m from the shoreline. The tidal flow with peak flood velocities of about 0.7 m/s to the north-east and peak ebb velocities of about 0.6 m/s to the south-west is parallel to the coast (**Figure 4.2.2**) and thus normal to the sand wave crest.

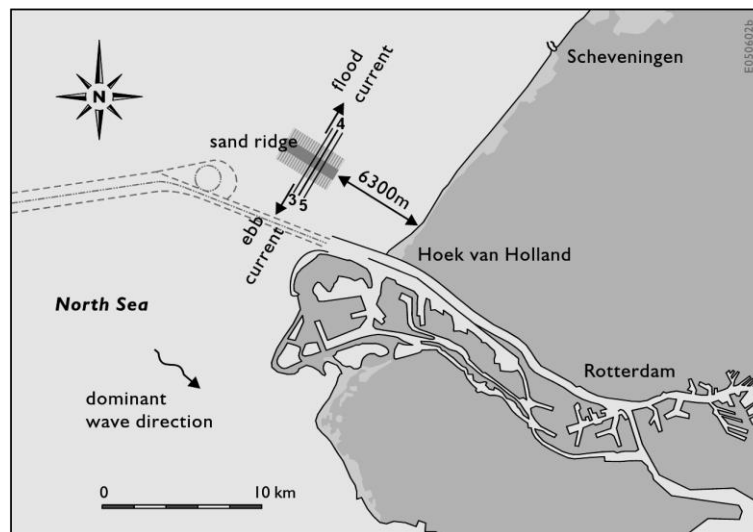


Figure 4.2.1 Plan view location of the artificial sand wave Hoek van Holland.

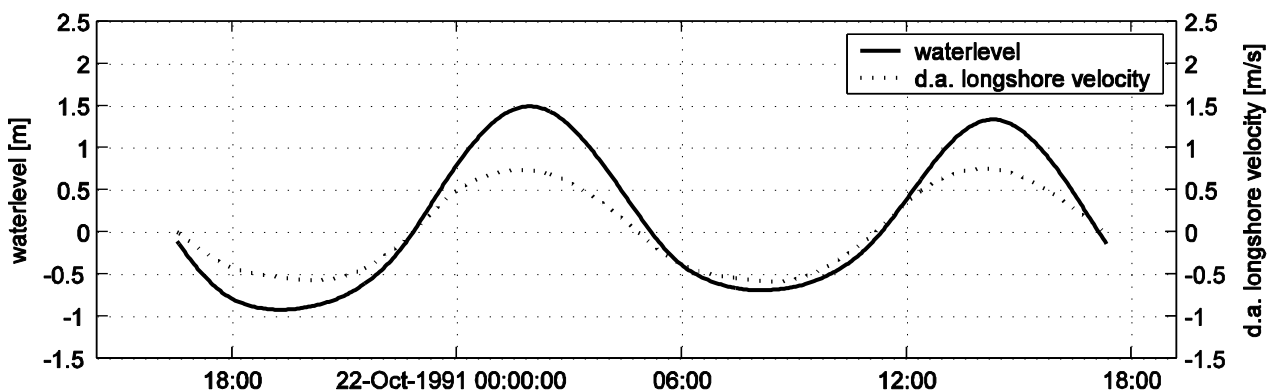


Figure 4.2.2 Computed horizontal (depth-averaged velocity) and vertical tide (water level) at a depth of 18 m at location Hoek van Holland.

Figure 4.2.2 shows the computed horizontal and vertical tide at a depth of 18 m at location Hoek van Holland, two and a half days before springtide. The daily inequality with water levels varying between -1m and 1.5m



is shown and it can be seen that there is only a very small phase difference between the horizontal and vertical tide in deeper water.

Between 1982 and 2000 bathymetric surveys of the artificial sand wave were carried out by Directorate North Sea (DNZ) of Rijkswaterstaat. Data collection before 1991 was carried out using the single-beam method, while data collection after 1991 was carried out using the more accurate multi-beam method. The vertical accuracy of the soundings is of the order of 0.1 to 0.2 m; the horizontal accuracy is of the order of 1 to 5 m.

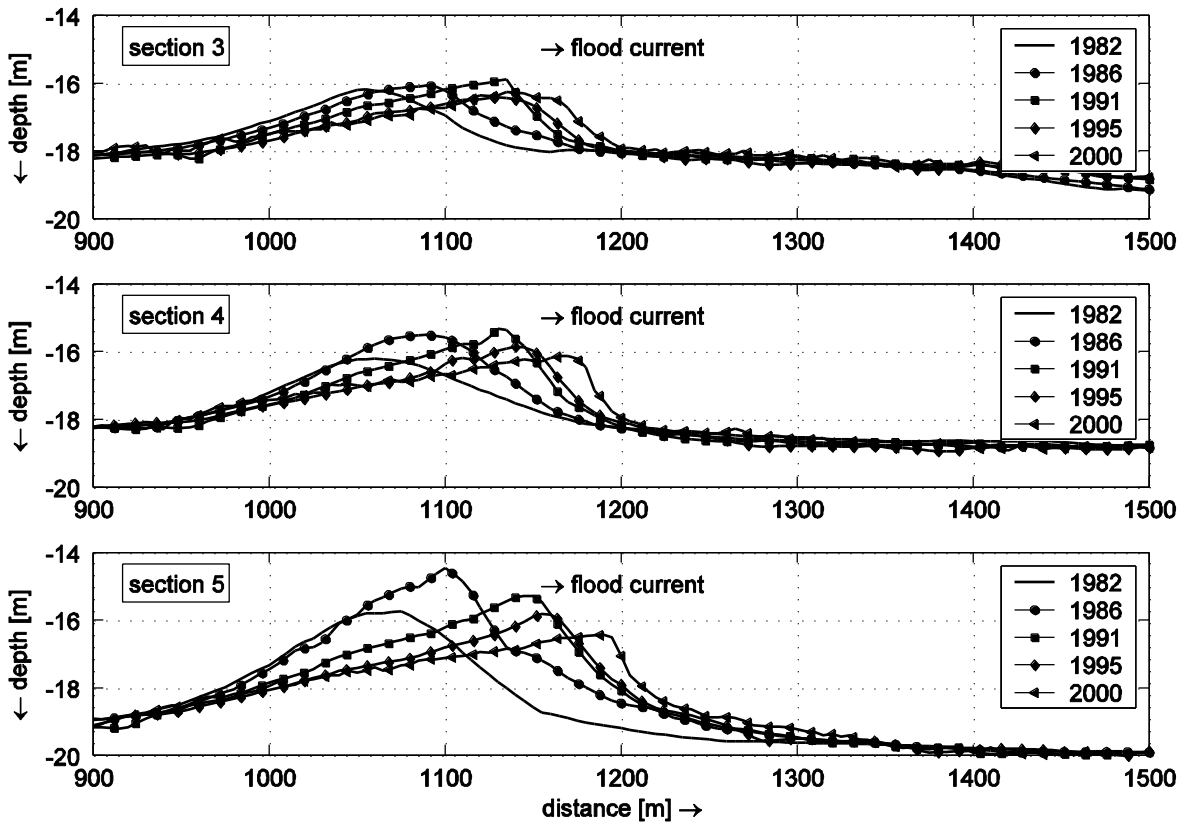


Figure 4.2.3 Measured bed levels for cross-sections 3, 4 and 5 (see Figure 4.2.1).

Figure 4.2.3 shows measured bed levels for cross-sections 3, 4 and 5 for the period 1982 – 2000. Between 1982 and 1986 the sand dumpings contributed to the vertical growth of the sand wave. Measurements for the period 1986 - 2000 show a clear reduction in sand wave height and a net migration of the crest in northern (flood) direction. Since the migration rate decreases with depth (18 m in cross-section 4 to about 25 m in cross-section 9), the sand wave shows a slight rotation with respect to the original axis. The base of the sand wave hardly changes over a period of 15 years. Hence, the shape of the sand wave is modified slightly (more asymmetric). The average rate of migration of the crest in the flood direction to the north-east is about 5.5 m per year and the average decrease in height is about 0.1 m per year (period 1982 to 2000).

The SEDTUBE-model has been used to simulate the migration of the artificial sand wave, see input data of Table 4.2.1 and the computed results of Figure 4.2.4. The flood and ebb depth-averaged velocities are 0.7 and 0.63 m/s. The sea bed consists of sand with  $d_{50} = 0.35$  mm. The annual-mean significant wave height is set to 1.2 m. The bed roughness is said to 0.01 m.

The computed migration over 2 years is about 15 m or 7.5 m/year, which is somewhat larger than the observed value of 5.5 m/year.

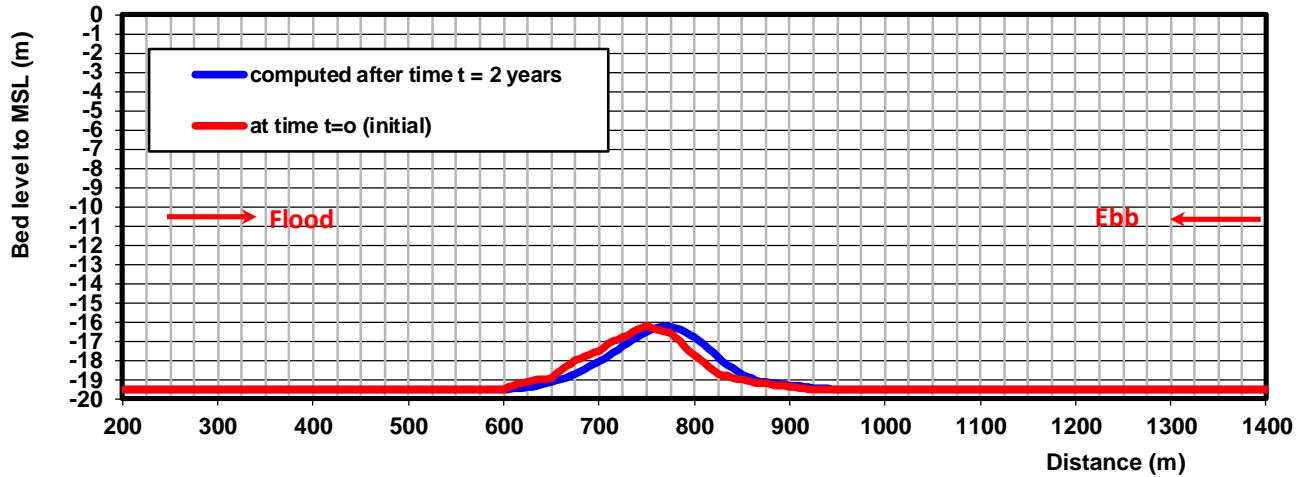


Figure 4.2.4 Computed migration of artificial sand wave near Hoek van Holland

<b>INPUT VALUES IN RED</b>			
<b>(columns E40 and F40 are also input data)</b>			
	<b>flood</b>	<b>eb</b>	
Depth-averaged velocity at x=0	<b>0.7</b>	<b>0.63</b>	(m/s)
Tidel level	<b>1.5</b>	<b>-1</b>	(m)
Wave height	<b>1.2</b>	<b>1.2</b>	(m)
Wave period	<b>7</b>	<b>7</b>	(s)
d50 of sand fraction		<b>0.00035</b>	(m)
d90 of sand fraction		<b>0.0006</b>	(m)
Fraction of mud in bed (range of 0 to 0.2)		<b>0.05</b>	(-)
Fluid density		<b>1020</b>	(kg/m <sup>3</sup> )
Sediment density		<b>2650</b>	(kg/m <sup>3</sup> )
Kinematic viscosity		<b>0.000001</b>	(m <sup>2</sup> /s)
Ws suspended sand		<b>0.045</b>	(m/s)
Bed Roughness ks		<b>0.01</b>	(m)
Porosity of bed material p		<b>0.4</b>	(-)
Calibration factor sand transport		<b>0.33</b>	(-)
Calibration factor critical velocity		<b>1</b>	(-)
Slope factor (0 to 1; Default=0=no effect)		<b>0.2</b>	(-)
Smoothing factor bed levels		<b>0.01</b>	(-)
Flow Duration Dt		<b>24</b>	(hours)
Grid size DX		<b>5</b>	(m)
Coefficient of adjustment factor (range 0.05-0.2)		<b>1</b>	(-)
Number of time steps for half a tide		<b>↑</b>	(-)
Total number of complete tides (= 2 half tides)		<b>180</b>	(-)

Table 4.2.1 Input data of SEDTUBE-model for artificial sand wave near Hoek van Holland



## 5. References

- Hulscher, S., 1996a.** Formation and migration of large-scale, rhythmic sea-bed patterns: a stability approach. Doctoral Thesis, Department of Oceanography, University of Utrecht, The Netherlands
- Hulscher, S., 1996b.** Tidal-induced large-scale regular bed form patterns in a three-dimensional shallow water model. *Journal of Geophysical Research*, Vol. 101, No. C9, p. 20727-20744
- Huthnance, J., 1982.** On one mechanism forming linear sand banks. *Estuarine Coastal shelf Science*, Vol. 4, p. 79-99
- Lesser, G., Roelvink, J.A., Van Kester, J.A.T.M. and Stelling, G.S., 2004.** Development and validation of a three-dimensional morphological model. *Journal of Coastal Engineering* Vol. 51, pp 883-915.
- Meene, J.W.H., 1994.** The shoreface-connected ridges along the central Dutch coast. Doctoral Thesis, Department of Physical Geography, University of Utrecht, The Netherlands
- Tonnon, P.K., Van Rijn, L.C. and Walstra, D.J.R., 2007.** The morphodynamic modelling of tidal sand waves on the shoreface. *Coastal Engineering* 54, 279-296
- Van Rijn, L.C., 1984.** Sediment transport, Part II: Suspended load transport. *Journal of Hydraulic Engineering*, ASCE, Vol. 110, No. 10
- Van Rijn, L.C., 1987.** Mathematical modelling of morphological processes in the case of suspended sediment transport. Doctoral Thesis, Department of civil engineering, Technical University of Delft, Delft, The Netherlands.
- Van Rijn, L.C., 1993, 2006.** Principles of sediment transport in rivers, estuaries and coastal seas. Aqua Publications, The Netherlands ([www.aquapublications.nl](http://www.aquapublications.nl))
- Van Rijn, L.C., 2007.** A unified view of sediment transport by currents and waves, Part I, II, III, *Journal of Hydraulic Engineering*, ASCE, No. 6, 649-667, 668-689; No. 7, 761-775
- Van Woudenberg, C.C., 1996.** Artificial sand wave at location Hoek van Holland (in Dutch). MSc Thesis/Report NZ-96-03, Dir. Noordzee, The Hague, The Netherlands.
- Vittori, G., Blondeaux, P., Hulscher, S.J.M.H., Piqueret, M. and Roos, P.C., 2005.** Potential use of sand waves and sand banks for sand mining, Paper K in: Sandpit, sand transport and morphology of offshore sand mining pits, edited by Van Rijn et al. Aqua Publications, The Netherlands ([www.aquapublications.nl](http://www.aquapublications.nl))